Restoration of solar and star images with phase diversity-based blind deconvolution

Qiang Li (李 强)[1,2], Sheng Liao (廖 胜)[1], Honggang Wei (魏宏刚)[1], and Mangzuo Shen (沈忙作)[1]

[1] *State Key Laboratory of Optical Technologies for Microfabrication, Institute of Optics and Electronics, Chinese Academy of Sciences, Chengdu 610209*

[2] *Graduate School of the Chinese Academy of Sciences, Beijing 100039*

Received November 16, 2006

The images recorded by a ground-based telescope are often degraded by atmospheric turbulence and the aberration of the optical system. Phase diversity-based blind deconvolution is an effective post-processing method that can be used to overcome the turbulence-induced degradation. The method uses an ensemble of short-exposure images obtained simultaneously from multiple cameras to jointly estimate the object and the wavefront distribution on pupil. Based on signal estimation theory and optimization theory, we derive the cost function and solve the large-scale optimization problem using a limited memory Broyden-Fletcher-Goldfarb-Shanno (L-BFGS) method. We apply the method to the turbulence-degraded images generated with computer, the solar images acquired with the swedish vacuum solar telescope (SVST, 0.475 m) in La Palma and the star images collected with 1.2-m telescope in Yunnan Observatory. In order to avoid edge effect in the restoration of the solar images, a modified Hanning apodized window is adopted. The star image still can be restored when the defocus distance is measured inaccurately. The restored results demonstrate that the method is efficient for removing the effect of turbulence and reconstructing the point-like or extended objects.

OCIS codes: 100.3020, 100.5070, 100.3190, 110.6770.

As light propagates through the atmosphere, light rays are distorted due to random variations in the index of refraction caused by atmospheric turbulence. This causes degradation of the images of astronomical object captured with a ground-based telescope. A variety of image restoration approaches have been developed to reduce or remove the turbulence-induced blurring. These approaches include speckle imaging[1,2], blind deconvolution[3], deconvolution with wavefront sensing[4,5], and phase diversity[6−8]. The concept of phase diversity was first proposed by Gonsalves[6] and extended by Paxman[7] *et al.*.

Phase diversity method is a technique for obtaining estimates of both the object and the distribution of wavefront induced by atmospheric turbulence. The technique requires the simultaneous collection of two or more short-exposure images. One of these images is the focal-plane image that has been degraded by unknown aberration, such as turbulence and telescope optical aberration. The other of these images is collected in a separate channel that is formed by further blurring the focal-image in some known fashion, such as by adding defocus. This can be accomplished with simple optical hardware, as shown in Fig. 1.

Incoherent isoplanatic imaging can be modeled as a linear shift-invariant process so that image formation is represented by a convolution

$$i_{tk}(x) = o(x) * h_{tk}(x) + n_{tk}(x),$$
$$t = 1, \cdots, T,\ k = 1, \cdots, K, \tag{1}$$

where $o(x)$ is the true object intensity distribution, $h_{tk}(x)$ is the point-spread function (PSF) of imaging system for tth frame and kth channel, $i_{tk}(x)$ is the corresponding image recorded by the detector, $n_{tk}(x)$ represents the additive noise, $*$ denotes two-dimensional (2D) convolution, x is a 2D vector in image plane, T denotes the number of time frames, and K denotes the number of phase diversity channels. We assume that we have T short-exposure image pairs, corresponding to T frames and K channels, typically K equals 2, as described in Fig. 1.

Under the near-field approximation, the PSF associated with the focused image is given by

$$h_{t1}(x) = \left| F^{-1}\left\{ P(u) \mathrm{e}^{i\phi_t(u)} \right\} \right|^2, \tag{2}$$

where u is a 2D vector in the pupil plane, ϕ_t is the unknown time-varying phase function, P is the binary aperture function, and $F^{-1}\{\cdots\}$ denotes the inverse Fourier transform. In the defocus plane, the PSF is given by

$$h_{t2}(x) = \left| F^{-1}\left\{ P(u) \mathrm{e}^{i[\phi_t(u)+\theta(u)]} \right\} \right|^2, \tag{3}$$

where θ is the phase diversity function. In general, θ can be any known function, such as defocus, astigmatism,

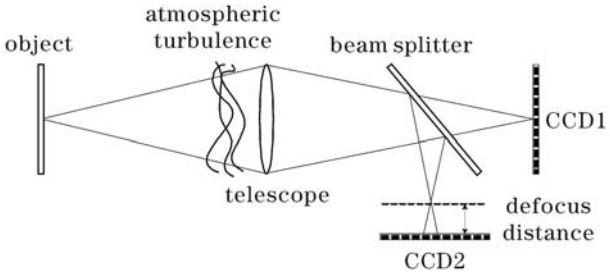

Fig. 1. Optical layout for phase diversity method.

1671-7694/2007/040201-03

coma, etc.. In this study, we adopt defocus as phase diversity function that can be described by

$$\theta(u) = c(u_x^2 + u_y^2), \tag{4}$$

where u_x and u_y are the normalized vectors in pupil plane, and c is the defocus coefficient dependent on the central wavelength λ, the defocus length d, the effective aperture D, and the focal length F through

$$c = \frac{2\pi}{\lambda}\frac{d}{8(F/D)^2}. \tag{5}$$

From Eqs. (1), (2) and (3), the image restoration problem is to estimate the unknown parameters (the object o and the phase function ϕ_t) from the data (focused i_{t1} and defocused i_{t2} images). If the additive Gaussian noise model is adopted[7], the object o and the phase function ϕ_t can be computed by minimizing the cost function[9]

$$J_0(o, \vec{\phi}) = \frac{1}{2}\left(\sum_{t=1}^{T}\sum_{k=1}^{K}\|o * h_{tk} - i_{tk}\|^2\right) + \frac{\gamma}{2}\|o\|^2, \tag{6}$$

where $\vec{\phi} = (\phi_1, \cdots, \phi_t, \cdots, \phi_T)$ and $\|\cdots\|$ denotes the Frobenius norm[10], the term $\|o\|^2$ is the regularization function whose purpose is to establish numerical stability with respect to perturbation in object o, the γ is the nonnegative scalar regularization parameter.

Using the convolution theorem and Parseval theorem, one can express J_0 in frequency domain

$$J_0(O, \vec{\phi}) = \frac{1}{2}\left(\sum_{t=1}^{T}\sum_{k=1}^{K}\|OH_{tk} - I_{tk}\|^2\right) + \frac{\gamma}{2}\|O\|^2, \tag{7}$$

where $O = F\{o\}$, $H_{tk} = F\{h_{tk}\}$, $I_{tk} = F\{i_{tk}\}$. Here $F\{\cdots\}$ denotes the Fourier transform. Setting to zero the derivative of J_0 with respect to O, one obtains the solution of O, as

$$O(\vec{\phi}) = \frac{\sum_{t=1}^{T}\sum_{k=1}^{K} H_{tk}^* I_{tk}}{\gamma + \sum_{t=1}^{T}\sum_{k=1}^{K}|H_{tk}|^2}, \tag{8}$$

here, the superscript $*$ denotes the complex conjugate. Note that the parameter γ in the denominator of Eq. (8) induces stability by preventing division by very small quantities or zero. By substituting O from Eq. (8) back into Eq. (7), one obtains the reduced cost function[9]

$$J(\vec{\phi}) = \frac{1}{2}\left(\sum_{t=1}^{T}\sum_{k=1}^{K}\|I_{tk}\|^2 - \left\|\frac{\sum_{t=1}^{T}\sum_{k=1}^{K} I_{tk}^* H_{tk}}{\gamma + \sum_{t=1}^{T}\sum_{k=1}^{K}|H_{tk}|^2}\right\|^2\right). \tag{9}$$

To minimize the reduced cost function $J(\vec{\phi}^m)$, we will use a quasi-Newton method known as limited memory Broyden-Fletcher-Goldfarb-Shanno (L-BFGS)[11]. The L-BFGS algorithm for minimization of Eq. (9) takes the form of the iteration

$$\vec{\phi}^{m+1} = \vec{\phi}^m - B(\vec{\phi}^m)^{-1} g(\vec{\phi}^m), \quad m = 0, 1, \cdots, \tag{10}$$

where $g(\vec{\phi}^m)$ is the gradient of $J(\vec{\phi}^m)$, $B(\vec{\phi}^m)$ denotes the approximation to Hessian (matrix of second partial derivatives) of $J(\vec{\phi}^m)$[11], m is the number of iterations. In Eq. (10), the formula of gradient function $g(\vec{\phi}^m)$ is available in Refs. [7, 9] and $B(\vec{\phi}^m)$ can be computed by using BFGS formula[11]. Therefore the phase diversity algorithm consists of the following step: Step 1. Set initial guess $\vec{\phi}^0 = 0$ and the number of iterations $m = 0$; Step 2. Compute $J(\vec{\phi}^m)$ and $g(\vec{\phi}^m)$; Step 3. Call optimization algorithm L-BFGS and estimate new solver $\vec{\phi}^{m+1}$ according to Eq. (10), $m = m + 1$; Step 4. If the stopping criterion is satisfied, compute the object o using Eq. (8) and go to end; if not, go back to Step 2. In Step 4, the algorithm will terminate when the change in the reduced cost function J is sufficiently small or the number of iterations m reaches the set value.

In order to ascertain the performance of the phase diversity algorithm, we applied it to one simulated dataset of computer-generated object and two real datasets of astronomical object. The first of real datasets is an extended object and the second is a point-like object.

We simulate the random phase screens according to von Karman turbulence model, and then generate multiple pairs of turbulence-degraded images[1]. The simulated parameters are as follows: the effective aperture D is 1.28 m, the focal length F is 40.0 m, the filter central wavelength λ is 600 nm, the defocus coefficient c is 1.0 wave, the atmospheric seeing parameter r_0 is 0.1 m, and the signal to noise ratio (SNR) is 25 dB. The true object, the turbulence-degraded in-focus image and out-of-focus image are shown in Figs. 2(a)—(c), respectively. Figure 2(d) shows the restored result obtained from eight image pairs after 500 iterations.

The dataset of extended object used in this section was the solar granulation data collected with Swedish vacuum solar telescope (SVST) in La Palma, 1993 April 27. The important parameters of the dataset are as follows: D is 0.475 m, F is 22.35 m, λ is 469.6 nm, and c is 0.985 waves[12]. When images are not periodic or bounded, using discrete Fourier transform to represent convolution will arise edge effect or ringing. In order to avoid this

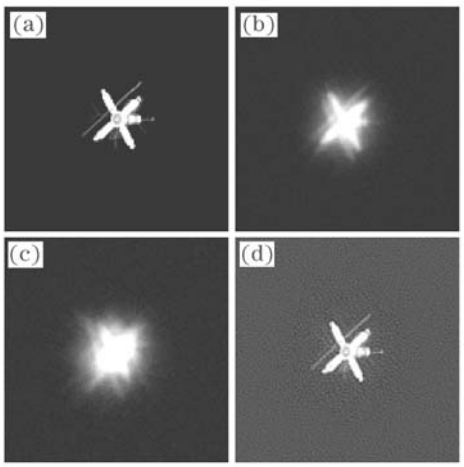

Fig. 2. Simulated turbulence-degraded images. (a) True object; (b) in-focus image; (c) out-of-focus image; (d) restored result using 8 image pairs.

Fig. 3. Short-exposure images of solar collected with SVST. (a) In-focus image; (b) out-of-focus image; (c) restored result using 8 image pairs.

effect, the 128×128 images were apodized with a 2D modified Hanning window where the apodized part extended over only 20 pixels near the boundaries. Figure 3(a) shows one typical in-focus image. Figure 3(b) shows one out-of-focus image collected with Fig. 3(a) at the same time. Figure 3(c) shows the restored result using eight image pairs after 600 iterations (including those shown in Figs. 3(a) and (b)). In Fig. 3, only 70×70 center region is displayed, which corresponds to the most reliable region after apodizing preprocess. In Fig. 3(c), we can found more fine details than in Fig. 3(a), such as the small granulation in the central region of restored image.

The dataset of point-like object was acquired with 1.2-m telescope in Yunnan Observatory. Some important observational parameters are as follows: D is 1.06 m, λ is 700.0 nm. A detail description of this telescope can be found in Ref. [13]. One typical image pair from a multiframe observation of single star is shown in Fig. 4, where Fig. 4(a) is in-focus image and Fig. 4(b) is out-of-focus image. The known defocus distance is essential to obtain accurate results, but in this experiment it is not measured accurately. It is shown that the defocus coefficient c varying from 0.5λ to 1.5λ provides accurate result[14]. In this study, the reduced cost function J is minimal when the defocus coefficient c is equal to

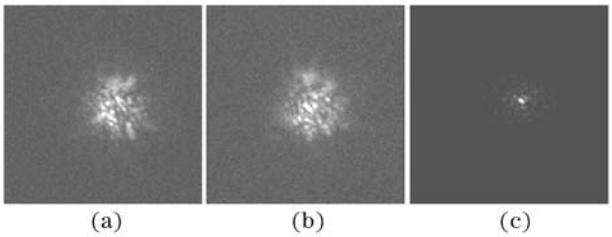

Fig. 4. Short-exposure images of single star collected with 1.2-m telescope in Yunnan Observatory. (a) In-focus image; (b) out-of-focus image; (c) restored result using 8 image pairs.

0.8 waves, which means we get the best result at this time. Figure 4(c) shows the restored result obtained from eight image pairs after 500 iterations.

In conclusion, the restored result of computer-generated object suggests the effectivity of the phase diversity-based blind deconvolution. Using the method, we have successfully restored the solar images acquired with SVST and the star images collected in Yunnan Observatory. Some fine details that are not visual in raw solar image have been founded in restored image. Although the defocus distance was not measured accurately, the degraded star images have been restored. The restored results demonstrate that the method is efficient for restoring turbulence-degraded images of the point-like and extended object.

The authors are grateful to Dr. M. G. Löfdahl of Institute for Solar Physics of the Royal Swedish Academy of Sciences for providing the solar dataset with SVST. This work was supported by the National "863" Program of China under Grant No. 8632774. Q. Li's email address is lleeqiang@yahoo.com.cn.

References

1. L. Yang and M. Shen, Opto-Electron. Eng. (in Chinese) **27,** (4) 7 (2000).
2. L. Yang and M. Shen, Proc. SPIE **4548,** 45 (2001).
3. T. J. Schulz, J. Opt. Soc. Am. A **10,** 1064 (1993).
4. Y. Liang, C. Rao, M. Li, and Z. Geng, Chin. Opt. Lett. **4,** 187 (2006).
5. L. M. Mugnier, C. Robert, J.-M. Conan, V. Michau, and S. Salem, J. Opt. Soc. Am. A **18,** 862 (2001).
6. R. A. Gonsalves, Opt. Eng. **21,** 829 (1982).
7. R. G. Paxman, T. J. Schulz, and J. R. Fienup, J. Opt. Soc. Am. A **9,** 1072 (1992).
8. J. Bardsley, S. Jefferies, J. Nagy, and R. Plemmons, Opt. Express **14,** 1768 (2006).
9. C. R. Vogel, T. Chan, and R. Plemmons, Proc. SPIE **3353,** 994 (1998).
10. G. H. Golub and C. F. Van Loan, *Matrix Computations* (The Johns Hopkins University Press, London, 1996) p.55.
11. R. H. Byrd, P. Lu, J. Nocedal, and C. Zhu, SIAM J. Sci. Comput. **16,** 1190 (1995).
12. M. G. Löfdahl and G. B. Schärmer, Astronomy and Astrophysics Supplement Series **107,** 243 (1994).
13. Y. Xiong and H. Fu, Opto-Electron. Eng. (in Chinese) **25,** (Suppl.) 66 (1998).
14. L. Meynadier, V. Michau, M.-T. Velluet, J.-M. Conan, L. M. Mugnier, and G. Rousset, Appl. Opt. **38,** 4967 (1999).